Impact of WAMS Malfunction on Power System Reliability Assessment

Farrokh Aminifar, *Member, IEEE*, Mahmud Fotuhi-Firuzabad, *Senior Member, IEEE*, Mohammad Shahidehpour, *Fellow, IEEE*, and Amir Safdarian, *Student Member, IEEE*

***Abstract*—Monitoring/control infrastructures are often assumed to be fully reliable in power system reliability studies. However, recent investigations on blackouts have revealed the crucial impacts of monitoring/control system malfunctions. This paper addresses the impact of situational awareness and controllability on power system reliability assessment. A methodology is proposed to simulate a situation in which a limitation of either or both monitoring and control functions could spread the consequence of power system events throughout the grid. It is assumed that the monitoring/control infrastructure is based on a wide-area measurement system (WAMS). While the proposed methodology is applicable to a variety of strategies for grid operations, certain assumptions are made for the simulation purposes. The Monte Carlo simulation is applied and a scenario reduction technique is considered for overcoming computational burdens. The performance of the proposed approach is simulated and analyzed on 9-bus and the IEEE 57-bus systems.**

***Index Terms*—Composite system reliability assessment, observability analysis, phasor measurement unit (PMU), wide-area measurement system (WAMS).**

NOMENCLATURE

A. Indices and Sets

i	Unit index.
l	Line index.
n	Bus index.
s	Scenario index.
s^p	Scenario index for power system.
s^w	Scenario index for WAMS.
B	Set of buses.
CB	Set of buses with controllable units and loads.
G_n	Set of units connected to bus n.
L	Set of lines.
OL	Set of observable lines.
S	Set of scenarios comprising monitoring/control and power system contingencies.
S^p	Set of scenarios for power system contingencies.
S^w	Set of scenarios for WAMS contingencies.

B. Parameters

x_l	Reactance of line l.
A_{nl}	Element of network incidence matrix, 1 when bus n is the sending bus of line l, -1 when bus n is the receiving bus of line l, 0 otherwise.
P_i^{bc}	Generating power of unit i in the base scenario.
$\bar{P}_i$, $\underline{P}_i$	Maximum and minimum capacity limits of unit i.
PD_n	Power demand at bus n.
$\overline{PF_l}$	Capacity of line l.
SL_i^s	Binary number representing state of line l in scenario s.
SU_i^s	Binary number representing state of unit i in scenario s.

C. Functions and Variables

$EDNS_n$	Expected demand not served at bus n.
$EDNS$	Expected demand not served of the entire system.
$f^s(\cdot)$	Objective function in OLS of scenario s.
LS_n^s	Load shed at bus n in scenario s.
PF_l^s	Power flow of line l in scenario s.
δ_n^s	Voltage phase angle of bus n in scenario s.
ΔP_i^s	Power redispatch of unit i in scenario s.

I. INTRODUCTION

INVESTIGATIONS conducted following the occurrences of large events in power grids have revealed the indispensible role of critical information at control centers and the impact of situational awareness on managing power system operations. In many occasions, the impact of outages could have been prevented or significantly reduced if system operators had a more complete knowledge on the corresponding state of stressed power systems [1].

Manuscript received August 21, 2011; revised November 27, 2011; accepted January 02, 2012. Date of publication March 16, 2012; date of current version August 20, 2012. This work was supported by the Iran National Science Foundation and is acknowledged by the first two authors. Paper no. TSG-00382-2011.

F. Aminifar, M. Fotuhi-Firuzabad, and A. Safdarian are with the Center of Excellence in Power System Control and Management, Electrical Engineering Department, Sharif University of Technology, Tehran, Iran (e-mail: frkh_aminifar@ee.sharif.edu; fotuhi@sharif.edu; a_safdarian@ee.sharif.edu).

M. Shahidehpour is with the Electrical and Computer Engineering Department, Illinois Institute of Technology, Chicago, IL 60616 USA (e-mail: ms@iit.edu).

Color versions of one or more of the figures in this paper are available online at http://ieeexplore.ieee.org.

Digital Object Identifier 10.1109/TSG.2012.2183397

Synchrophasor measurement technology (SMT) was recognized as a promising alternative for enhancing the situational awareness. It provides an unprecedented insight on the real-time state of power systems with a wide-area coverage [1]–[3]. Phasor measurement units (PMUs) are the building block of SMT [3]. SMT, which is also referred to as wide-area measurement system (WAMS), is presently accounted for monitoring and control of static and dynamic power systems.

In the literature, few studies focused on the role of monitoring/control infrastructures in the probabilistic power system reliability assessment. Reference [4] reported a probabilistic case study on the overall reliability of control center facilities in Ontario Hydro. The paper considered failures in control center equipment; however, it did not study malfunctions associated with the supervisory control and data acquisition (SCADA) system and their impacts on power system performance. A joint SCADA and power system model was considered in [5] in which the impact of SCADA failures on power system load curtailments was analyzed. The idea was valuable; however, the approach was not elaborated on its details. The paper presented limitations on controllability but did not incorporate observability deficits in power system analyses.

The WAMS applications were examined in [6] using simple examples. The probability of successful operations was calculated based on the availability of WAMS elements. However, the probabilistic power system analyses were preliminary. Reference [7] conducted the calculation of multiple reliability indices for a regional network of WAMS. The outages of PMUs and communication links were considered, while those of other key components such as measuring transformers or transmission lines were excluded. The authors extended their works in [8] by presenting a quantitative reliability evaluation method for the communication network of WAMS and the overall WAMS from a hardware reliability perspective.

In [9], the observability of WAMS-based power networks was analyzed from a probabilistic viewpoint. A probabilistic observability index was introduced for buses associated with a PMU placement configuration. The average of bus indices represented a system index with an insight on the overall network observability. The proposed model in [9] was extended in [10]; however, both studies were devised with the intention of PMU placement in power systems. References [6]–[10] studied the WAMS performance as a single system; however, they did not investigate the impact of WAMS failures on power system performance analyses.

In this paper, the proposed methodology considers WAMS as a viable monitoring/control infrastructure in electric power systems. This assumption is due to straightforward observability rules embedded in the WAMS model. The WAMS application to the enhancement of power system operation is discussed and requirements for the joint reliability assessment of WAMS and power system infrastructures are identified. As reliability analyses assess the performance of static power systems, the WAMS capability in monitoring power system dynamics is not modeled here. This feature makes the proposed framework applicable in the SCADA-based power systems where the supply-demand balance and transmission system loading are just monitored. A set of assumptions in the proposed study represent the complexity of the problem which is, in turn, due to miscellaneous infrastructures deployed across the world.

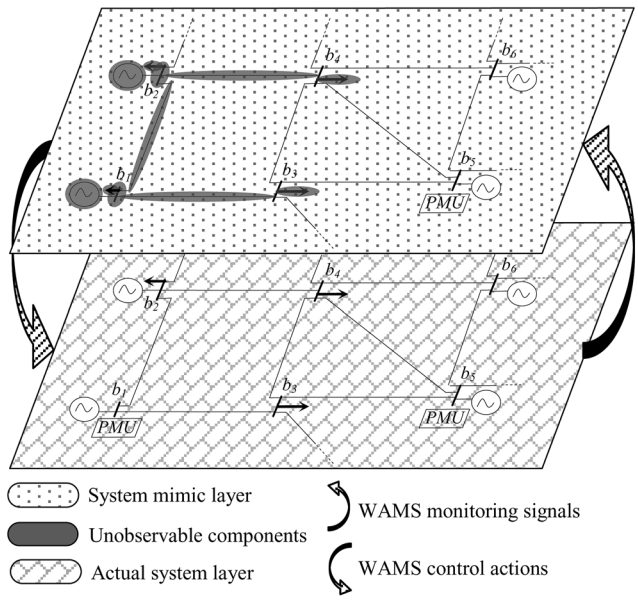

Fig. 1. Actual power system and mimic diagram.

However, such assumptions would be tailored for other WAMS cases. For instance, WAMS is assumed in the paper to be the key entity in charge of monitoring and control functions for power system reliability studies. However, other options for the monitoring and control in power systems are discussed and simulated as well.

Next, the proposed methodology which incorporates WAMS malfunctions in the power system reliability evaluation is devised. The outline of the algorithm is followed by the step by step procedure for the implementation of the proposed approach and the detailed formulations of the algorithm. Numerical analyses are then conducted on a 9-bus system and the IEEE 57-bus test system and the results are analyzed further based on the assumptions presented throughout the paper.

II. Proposed Concepts

Contingency analysis in the reliability evaluation of power systems assumes a complete observability over the system faults and operation status. It also supposes specific remedial actions and applies load shedding as the last resort at any load points requested. These procedures imply a reliable monitoring and control system, which could be somewhat an unrealistic assumption.

In Fig. 1, a two-layer power system model is demonstrated. The lower layer implies the actual power system. The upper layer shows the mimic diagram in a control center. The WAMS is the interface between these two layers. When power system contingencies occur within an unobservable region, the operator would not be directly informed on the event and might only be able to monitor consequential changes in observable power system portions. Remedial actions applied to observable regions of power systems could shift the power system state where the unobservable region might experience further sever conditions. Such ill-conditioned actions could trigger cascading outages which might remain unknown to system operators. A realistic reliability assessment methodology should consider the entire modeling of the actual power system layer. Such an effort would be presented in the next section.

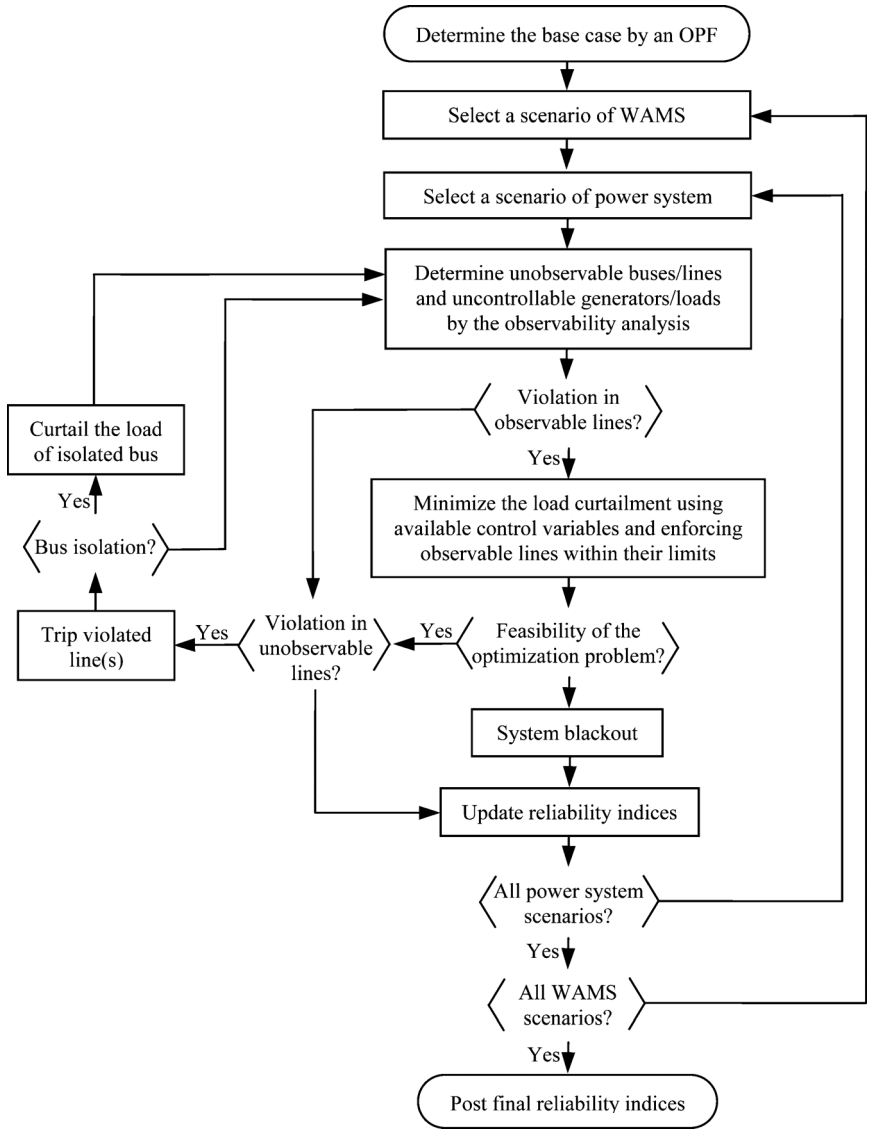

Fig. 2. Proposed algorithm for joint reliability evaluation of power system and WAMS.

We assume in the proposed approach that the protection system is perfect and focus our attention on WAMS failures. Such malfunctions could be accommodated in the extended version of the proposed reliability analyses.

III. Proposed Methodology

This section presents the proposed methodology for assessing the impact of WAMS malfunctions on the power system reliability assessment. The flowchart of the algorithm is depicted in Fig. 2. The procedure devised in this figure is as follows.

Step 1: The first step is to determine a base case OPF [11].

Step 2: The outer loop iterates on WAMS scenarios. The initial set of scenarios is truncated to a tractable level [12]. The composite power system reliability evaluation is conducted for each scenario.

Step 3: The inner loop considers power system scenarios in which the scenario reduction is applied again.

Step 4: An observability analysis accounts for forced outages in monitoring and power system levels [13], [14]. In this analysis, the PMU measurement of a given line current offers an indirect voltage measurement associated with the line other end. The observability rules are summarized as: i) a PMU located at a given bus would make itself and adjacent buses observable; ii) a transmission line with observable terminals is observable since its current and power flow could be calculated. The addition of PMUs and the provision of redundant communication channels would enhance the power system observability. Note as well that for SCADA-equipped power systems, this step merely represents the state estimation (SE). Assuming WAMS for both monitoring and control, this step will also identify uncontrollable parameters. In the event of any WAMS failures, the communication path between the control center and system buses could become partially unavailable. Accordingly, certain system variables would become uncontrollable. However, if the WAMS is only responsible for the system monitoring, we assume that the system is fully controllable for the sake of this study.

Step 5: With the event of violations in observable regions, the system operator will prescribe remedial actions for mitigating them. These actions are simulated by an optimal load shedding (OLS) optimization algorithm which will be outlined in this section.

Step 6: This step simulates the role of protection system in tripping out overloaded lines. Any violations in the unobservable region is checked at this step. In the case, the violated lines will be tripped by the protection system.

Step 7: The isolated buses are identified, their generating units are shut down, and the respective loads are curtailed. Since the system switches to a new operating point, the algorithm returns to Step 5 to check other violations.

Step 8: Reliability indices are updated based on load curtailments in scenario s and the probability of occurrence of this scenario.

A. Formulation

The OLS problem, in Step 5, is formulated in (1)–(8).

$$\min f^s = \sum_{n\in B} LS_n^s \tag{1}$$

Subject to

$$PF_l^s = \frac{SL_l^s}{x_l}\sum_{n\in B} A_{nl}\delta_n^s; \quad l \in L \tag{2}$$

$$\sum_{i\in G_n} SU_i^s(P_i^{bc}+\Delta P_i^s) - \sum_{l\in L} A_{nl}PF_l^s = PD_n - LS_n^s; \quad n \in B \tag{3}$$

$$-\overline{PF}_l \le PF_l^s \le \overline{PF}_l; \quad l \in OL \tag{4}$$

$$\underline{P}_i - P_i^{bc} \le \Delta P_i^s \le \bar{P}_i - P_i^{bc}; \quad i \in G_n,\ n \in CB \tag{5}$$

$$0 \le LS_n^s \le PD_n; \quad \forall n \in CB \tag{6}$$

$$\Delta P_i^s = 0; \quad \forall i \in G_n, \quad \forall n \in B - CB \tag{7}$$

$$LS_n^s = 0; \quad \forall n \in B - CB. \tag{8}$$

Here, the joint scenario set S for power system and WAMS comprises scenario sets S^w and S^p as

$$S = S^w \times S^p = \{s\} = \{(s^w, s^p) | s^w \in S^w \wedge s^p \in S^p\} \tag{9}$$

where $s \in S$ and (s^w, s^p) is an ordered pair of scenarios for WAMS and power system.

In each scenario, the objective is to minimize the load shedding in (1). The line flow calculation (2) has a binary parameter SL_l^s where 0 stands for the state of lines on outage making the power flow of such lines equal to 0. In (3), the bus-level power balance is considered and the units on outage are excluded by incorporating the binary parameter SU_i^s. The load shedding variable LS_n^s is considered in the power balance equation to make the problem feasible. The set of constraints (4) compels observable line flows to be within limits. The range of possible redispatch associated with controllable and uncontrollable generating units are determined by (5) and (7), respectively. Sets of constraints (6) and (8) declare the range of deployable load shedding associated with controllable and uncontrollable demands.

If WAMS is merely in charge of monitoring and the system control is managed through other media such as telephone lines, the proposed formulation will be modified slightly. Equation (1)–(3) will remain since they model the power flow problem in the given scenario. Also, as the system WAMS malfunctions still restrict the operator insight, the flow limits are met just in observable regions. So the set of constraints (4) will remain. In contrast, (5)–(6) will be formed for all buses, i.e., $\forall n \in B$, and (7)–(8) will be removed.

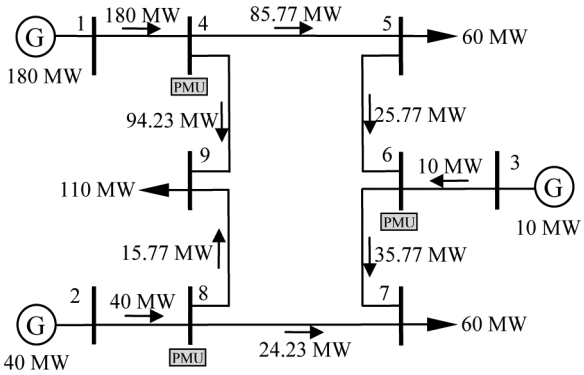

Fig. 3. Single-line diagram of the nine-bus system.

TABLE I
GENERATING UNIT DATA

	Unit located at bus		
	1	2	3
$\underline{P}_i$ [MW]	0	0	0
$\bar{P}_i$ [MW]	220	40	120
P_i^{bc} [MW]	180	40	10
Availability	0.98	0.96	0.99

TABLE II
SYSTEM DEMAND DISTRIBUTION

	Demand located at bus		
	5	7	9
PD_n [MW]	60	60	110
% total	26.09	26.09	47.82

TABLE III
TRANSMISSION SYSTEM DATA

Line		x_l [p.u.]	$\overline{PF}_l$ [MW]	Availability
From	To			
1	4	0.170	250	0.9907
2	8	0.143	120	0.9965
3	6	0.189	140	0.9942
4	5	0.085	110	0.9952
4	9	0.140	160	0.9943
5	6	0.206	110	0.9905
6	7	0.137	110	0.9976
7	8	0.241	55	0.9944
8	9	0.097	55	0.9954

IV. CASE STUDY AND DISCUSSIONS: A NINE-BUS SYSTEM

In this section, a nine-bus system is studied [9], [10], [13]. The nine-bus system with the base case power flow solution is depicted in Fig. 3. The data are given in Tables I–III.

As shown in Fig. 3, the WAMS network allocated for the system monitoring/control consists of three PMUs installed at buses 4, 6, and 8. These devices make the network fully observable, while buses 5, 7, 9 have redundant PMU measurements.

TABLE IV
WAMS COMPONENTS RELIABILITY DATA

Component	Availability
PMU [15]	0.995497
Current Transformer (CT) [16]	0.999584
Potential Transformer (PT) [16]	0.998542
Communication link [17]	0.999

TABLE V
CASE 1: RELIABILITY INDICES

	Load point bus			System
	5	7	9	
EDNS [MW]	0.386	0.178	1.699	2.263
% total	17.06	7.87	75.07	100

The reliability data of WAMS components are given in Table IV. For each phasor calculation, three-phase measurements are necessary [3]. So a PMU requires three CTs in the operating state for calculating a current phasor and the associated availability would be $(0.999584)^3$. The requirement for the voltage phasor is the same. The following cases are studied:

Case 1: Power system contingencies with reliable WAMS.
Case 2: Few joint contingencies of power system and WAMS.
Case 3: All contingencies of power system and WAMS.

A. Case 1

This case is the comparison benchmark to quantify the impact of WAMS malfunctions on the power system reliability indices. Table V gives the reliability indices for load points and the power system. Here, the largest load point index is at bus 9. The contribution of $EDNS_9$ to the system index is not well correlated with the ratio of PD_9 to the system demand (see Table II). In addition, $EDNS_5$ is much larger than $EDNS_7$ while $PD_5 = PD_7$. These observations are justified by load shedding procedure associated with contingencies.

B. Case 2

This case simulates a set of joint contingencies in power system and WAMS.

1) Contingency 1: PMU at bus 4 and line 1–4 (or generating unit at bus 1) are on outage. This contingency simulates the frequency instability and potential power blackout condition. In this contingency, the system generation capacity is 160 MW and, at least, 70 MW load shedding is required. Due to the WAMS malfunction, the system curtailable load is just 60 MW at bus 7. Accordingly, the demand exceeds the generation and the system frequency drops which will lead to a blackout. In practice, the automatic under-frequency protection could prevent such widespread impact of the disturbance. The protection model will be incorporated in the follow-up version of the proposed reliability analyses.

2) Contingency 2: PMU at bus 6 and line 1–4 are on outage. This contingency simulates the impact of WAMS availability on load shedding. From the power system viewpoint, this contingency is similar to Contingency 1. However, WAMS failure will influence other components. In Contingency 2, the load point at bus 9 and its linking transmission lines are controllable and observable, respectively. So the 70 MW loss of generation is balanced by a load shedding at bus 9.

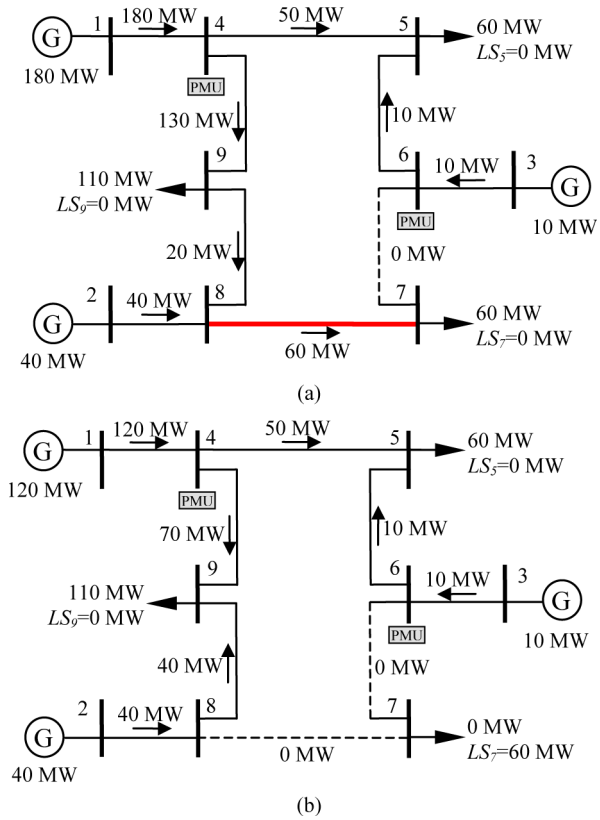

Fig. 4. Case 2, Contingency 3: load flow following line 6–7 outage. (a) Precascading outage. (b) Postcascading outage.

3) Contingency 3: PMU at bus 8 and line 6–7 are on outage. This contingency simulates cascading outages and bus isolation. The observability analysis shows buses 2, 7, 8 and lines 2–8, 7–8, 8–9 as unobservable. Fig. 4(a) shows the power flow solution once line 6–7 is on outage. Line 7–8 with a capacity of 55 MW is the only path to supply the 60 MW load at bus 7. So line 7–8 is overloaded while it is not observable in the control center. Consequently, the protection system trips line 7–8. The cascading event leaves bus 7 isolated in which the load will be curtailed. The curtailment of 60 MW load requires a reduction in generation dispatch of unit 1 by 120 MW. Fig. 4(b) shows the line flow in post-cascading outage. Based on the common reliability evaluation, the solution of this contingency would be $LS_7 = 5$ MW to relieve the line 7–8 overload regardless of its un-observation in the control center.

4) Contingency 4: The PMU at bus 8 and generating unit at bus 2 are on outage. This contingency simulates the situation that the faulted system remains healthy. Following the outage of generating unit 2, the system slack unit at bus 3 compensates the generation loss and the new power flow solution does not violate transmission limits. Table VI summarizes the load shedding results in Case 2.

C. Case 3

In this case, all contingencies associated with both power system and WAMS network are considered including four states analyzed in the previous case. Table VII gives the load points and system reliability indices. This case is comparable with Case 1 in which the WAMS network was assumed to be fully reliable. In Table VII, WAMS contingencies deteriorate

TABLE VI
CASE 2: LOAD CURTAILMENTS OF CONTINGENCIES 1–4

	LS_n at bus n [MW]		
	5	7	9
Contingency 1	60	60	110
Contingency 2	0	0	70
Contingency 3	0	60	0
Contingency 4	0	0	0

TABLE VII
COMPARISON OF RELIABILITY INDICES IN CASES 1 AND 3

	EDNS at bus n [MW]			System
	5	7	9	*EDNS*
Case 1	0.386	0.178	1.699	2.263
Case 3	0.417	0.215	1.747	2.379
Difference [%]	8.03	20.78	2.82	5.12

TABLE VIII
RELIABILITY INDICES WITH A RELIABLE WAMS

	Load point bus			System
	5	7	9	
Case 3	0.417	0.215	1.747	2.379
Multiplying factor = 0.1	0.389	0.181	1.707	2.277
Difference [%]	-6.71	-15.81	-2.28	-4.28
Multiplying factor = 10	0.663	0.524	2.142	3.329
Difference [%]	58.99	143.7	22.61	39.93

the system reliability. The load point reliability index varies in large interval ranging from 2.82 to 20.78%.

D. Impact of Key Parameters

1) Availability of WAMS Component Data: Two situations in Case 3 are examined here in which the unavailability of WAMS (see Table IV) is multiplied by a factor of 0.1 or 10. The former simulates an extremely reliable WAMS network. Table VIII shows the results which are compared with those of Case 3. The less reliable WAMS could deteriorate the power system reliability. Table VIII shows that load point indices vary in large intervals which is due to the OLS feasibility and its multiple solutions.

2) Deployment of Additional PMUs: In general, improving the component availability could be very costly or even infeasible. A more practical approach would be to incorporate redundant components [18]. In WAMS system, additional PMUs can be installed in a given bus to enhance the system observability in the event of either power system or WAMS outages. Accordingly, we consider 1 more PMU for the small nine-bus system. The additional PMU could be located at buses 1, 2, 3, 5, 7, and 9. So there are 6 solutions for the placement of 4 PMUs. Table IX presents the breakdown of reliability index for the base and new placement schemes. The improvement varies for different PMU schemes.

In Table IX, adding a PMU at bus 9 is the most effective solution since the system bulk load is connected to this bus. The second solution refers to an additional PMU at bus 1 which consists of the system largest generating unit. The next effective solution is the placement of PMUs at buses 4, 6, 7, and 8. In this solution, the major improvement occurs in $EDNS_7$ because bus 7 is equipped with the additional PMU and the chance of its isolation originated by line overloads significantly declines.

TABLE IX
RELIABILITY INDICES FOR VARIOUS PLACEMENT SCHEMES OF 4 PMUS

PMU equipped buses	*EDNS* at bus n [MW]			System
	5	7	9	*EDNS*
4, 6, 8	0.417	0.215	1.747	2.379
1, 4, 6, 8	0.402	0.199	1.728	2.329
2, 4, 6, 8	0.404	0.201	1.731	2.336
3, 4, 6, 8	0.420	0.217	1.742	2.379
4, 5, 6, 8	0.408	0.203	1.725	2.336
4, 6, 7, 8	0.408	0.202	1.724	2.334
4, 6, 8, 9	0.389	0.183	1.711	2.283

TABLE X
AVAILABILITY OF GENERATING UNITS

Unit connected to bus #	Availability
1	0.95
2	0.98
3	0.97
6	0.98
8	0.95
9	0.98
12	0.95

Hence, buses with large units and/or loads are better candidates for the PMU installation. However, if the value of lost load (VOLL) or synonymously interrupted energy assessment rate (IEAR) is considered in the power system reliability assessment, the buses serving economical or critical loads are suited for enhancing the observability.

V. CASE STUDY AND DISCUSSION: IEEE 57-BUS SYSTEM

In this section, the proposed reliability evaluation methodology is tested on the IEEE 57-bus system [9], [10], [13]. The system has 80 transmission lines, 7 generating units with 1975 MW generation capacity, and 42 bulk loads with 1250 MW demand. The data for the base case power flow solution are available at [19]. Generating units' data are taken from [19] and their availabilities are given in Table X. Line capacities are presented in Table XI and their availability data are taken from [9].

Fig. 5 depicts the IEEE 57-bus system and 17 PMUs for the WAMS network. The reliability data considered for the WAMS components are the same as those given in Table IV. The numerical simulations consist of the following cases:

Case 1: Power system contingencies with a reliable WAMS.

Case 2: All contingencies of power system and WAMS.

Case 3: Same as Case 2 but the controllability is fully reliable.

Table XII shows the system reliability index associated with the three case studies. The CPU time for the calculation of Case 2 was about 30 minutes on a Core i7 1.60-GHz processor and 4 GB of RAM.

$EDNS$ in Case 1 represents the system reliability based on the conventional evaluation analysis. $EDNS$ in Case 2 shows a 41% increase as compared with that of Case 1. So incorporating the malfunction of WAMS components, as expected, provides a more comprehensive system reliability index. In Case 3, it is assumed that WAMS is just in charge of system monitoring and control actions are rendered through another media which is not affected by WAMS failures. As expected, in this case, the system reliability index $(EDNS)$ is greater than that of Case

TABLE XI
CAPACITY OF TRANSMISSION LINES [MW]

From	To	$\overline{PF}_l$	From	To	$\overline{PF}_l$	From	To	$\overline{PF}_l$
1	2	125	14	15	135	41	42	80
2	3	165	18	19	90	41	43	90
3	4	165	19	20	80	38	44	115
4	5	110	21	20	100	15	45	85
4	6	100	21	22	100	14	46	95
6	7	125	22	23	90	46	47	100
6	8	90	23	24	115	47	48	90
8	9	80	24	25	100	48	49	105
9	10	75	24	25	100	49	50	90
9	11	70	24	26	105	50	51	100
9	12	65	26	27	80	10	51	85
9	13	85	27	28	90	13	49	75
13	14	135	28	29	70	29	52	100
13	15	165	7	29	110	52	53	95
1	15	225	25	30	90	53	54	90
1	16	165	30	31	95	54	55	80
1	17	175	31	32	80	11	43	100
3	15	165	32	33	100	44	45	95
4	18	115	34	32	75	40	56	60
4	18	115	34	35	95	56	41	70
5	6	100	35	36	70	56	42	80
7	8	80	36	37	65	39	57	65
10	12	110	37	38	70	57	56	95
11	13	100	37	39	85	38	49	85
12	13	115	36	40	75	38	48	110
12	16	100	22	38	80	9	55	115
12	17	125	11	41	55	-	-	-

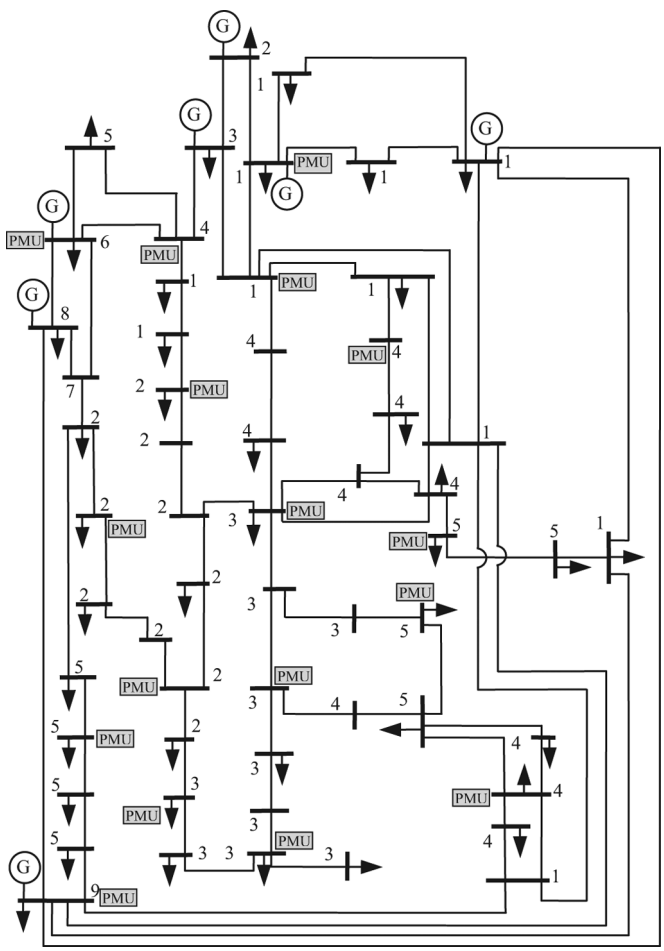

Fig. 5. IEEE 57-bus network with the given PMUs.

TABLE XII
SYSTEM $EDNS$ [MW]

Case 1	1.63
Case 2	2.30
Case 3	1.80

TABLE XIII
MAJOR LOAD POINT RELIABILITY INDICES IN CASE 2

Bus # n	PD_n [MW]	$EDNS_n$ [MW]
1	55	0.0219
3	41	0.0238
6	75	0.0293
8	150	0.0588
9	121	0.0493
12	377	1.8793
16	43	0.0175
17	42	0.0184
18	27.2	0.0118
47	29.7	0.0135

1. This is due to incorporating the observability deficits associated with WAMS malfunctions. On the contrary, comparison of Cases 2 and 3 reveals that accounting controllability deficits would further deteriorate the system reliability.

The following discussion is limited to Case 2 which is the major case study. Due to the large dimensions, it is not possible to present the results at all load points. So the major load point buses, with demands greater than 25 MW, are adopted and their respective reliability indices are detailed in Table XIII. For the sake of comparison, $EDNS$ reliability index is employed since load shedding amount directly influences this index. As shown in Table XIII, $EDNS_n$ of all buses, except bus 12, are in a same order of magnitude. The reason can be declared through analysis of the measurement robustness associated with buses 8, 9, and 12 as those serve largest loads. As depicted in Fig. 5, bus 8 is redundantly observable through two paths, namely PMUs at buses 6 and 9. Also, bus 9 is equipped with its own PMU and its observability is independent on the network topology. However, bus 12 is neither furnished with a PMU nor does it have redundant observability sources. So the probability of observability [10] of this bus is significantly lower than those of buses 8 and 9.

As a cascading event, the concurrent outages of PMU at bus 9 and line 1–17 is considered. Here, buses 9, 10, 11, 12, and 55 and all linking lines are unobservable. So the overloaded line 12–16 will trip. Thereafter, the overloaded line 12–13 will trip. The cascading event is ended when lines 8–9, 9–10, 9–11, 9–12, and 10–12 trip.

VI. CONCLUSIONS

This paper has enabled a methodology for incorporating WAMS malfunctions in power system reliability assessment. It was assumed that WAMS is in charge of the monitoring and/or control activities.

Based on numerical studies, the proposed method is able to model the situation in which the WAMS network suffers failures and an event in power systems would consequently spread out. Such events, although might be unlikely, could significantly

contribute to load shedding and simulate major changes in reliability assessments. These events are usually overlooked in conventional reliability evaluation studies. Numerical analyses show that buses with large generating units and loads should be candidates for PMU installations. It was deduced that, due to very long execution times, a few shortcuts should be devised to speed up the process. Scenario reduction was the approach adopted here while other alternatives such as parallel processing or running over pre-selected contingencies would also be possible. These studies underlined the indisputable role of information infrastructure on the power system adequacy evaluation. Other infrastructures such as the natural gas network and water resources could influence the problem as well and the joint analysis of all these systems should be considered in future studies.

REFERENCES

[1] "Real-time application of synchrophasors for improving reliability," North American Electric Reliability Corporation, 2010.

[2] V. Terzija, G. Valverde, C. Deyu, P. Regulski, V. Madani, J. Fitch, S. Skok, M. M. Begovic, and A. Phadke, "Wide-area monitoring, protection, and control of future electric power networks," *Proc. IEEE*, vol. 99, no. 1, pp. 80–93, Jan. 2011.

[3] G. Phadke and J. S. Thorp, *Synchronized Phasor Measurements and Their Applications*. New York: Springer, 2008.

[4] L. Wang, P. P. Gelberger, and N. Ramani, "Reliability assessment of the operational functions of a power system control center," *Proc. IET Prob. Methods Appl. Electr. Power Syst.*, pp. 229–234, Jul. 1991.

[5] A. G. Bruce, "Reliability analysis of electric utility SCADA systems," *IEEE Trans. Power Syst.*, vol. 13, no. 3, pp. 844–849, Aug. 1998.

[6] M. Zima, M. Larsson, P. Korba, C. Rehtanz, and G. Andersson, "Design aspects for wide-area monitoring and control systems," *Proc. IEEE*, vol. 93, no. 5, pp. 970–996, May 2005.

[7] Y. Wang, W. Li, J. Lu, and H. Liu, "Evaluating multiple reliability indices of regional networks in wide area measurement system," *Electr. Power Syst. Res.*, vol. 73, no. 10, pp. 1353–1359, Oct. 2009.

[8] Y. Wang, W. Li, and J. Lu, "Reliability analysis of wide-area measurement system," *IEEE Trans. Power Del.*, vol. 25, no. 3, pp. 1483–1491, Jul. 2010.

[9] F. Aminifar, M. Fotuhi-Firuzabad, M. Shahidehpour, and A. Khodaei, "Observability enhancement by optimal PMU placement considering random power system outages," *Energy Syst.*, vol. 2, no. 1, pp. 45–65, Mar. 2011.

[10] F. Aminifar, M. Fotuhi-Firuzabad, M. Shahidehpour, and A. Khodaei, "Probabilistic multistage PMU placement in electric power systems," *IEEE Trans. Power Del.*, vol. 26, no. 2, pp. 841–849, Apr. 2011.

[11] A. J. Wood and B. F. Wollenberg, *Power Generation, Operation, and Control*, 2nd ed. New York: Wiley, 1996.

[12] J. Dupacová, N. Gröwe-Kuska, and W. Römisch, "Scenario reduction in stochastic programming: An approach using probability metrics," *Math. Program.*, vol. A 95, pp. 493–511, 2003.

[13] F. Aminifar, A. Khodaei, M. Fotuhi-Firuzabad, and M. Shahidehpour, "Contingency-Constrained PMU placement in power networks," *IEEE Trans. Power Syst.*, vol. 25, no. 1, pp. 516–523, Feb. 2010.

[14] F. Aminifar, C. Lucas, A. Khodaei, and M. Fotuhi-Firuzabad, "Optimal placement of phasor measurement units using immunity genetic algorithm," *IEEE Trans. Power Del.*, vol. 24, no. 3, pp. 1014–1020, Jul. 2009.

[15] F. Aminifar, S. Bagheri-Shouraki, M. Fotuhi-Firuzabad, and M. Shahidehpour, "Reliability modeling of PMUs using fuzzy sets," *IEEE Trans. Power Del.*, vol. 25, no. 4, pp. 2384–2391, Nov. 2010.

[16] M. J. Rice and G. T. Heydt, "The measurement outage table and state estimation," *IEEE Trans. Power Syst.*, vol. 23, no. 2, pp. 353–360, May 2008.

[17] "Performance requirements task team (PRTT), performance requirements, Part II, Targeted applications: State estimation," Eastern Interconnection Phasor Project, 2005.

[18] H. Pham, *Handbook of Reliability Engineering*. New York: Springer, 2003.

[19] MATPOWER [Online]. Available: http://www.pserc.cornell.edu/matpower

Farrokh Aminifar (S'07–M'11) received the M.Sc. and Ph.D. degrees in electrical engineering from Sharif University of Technology, Tehran, Iran, in 2007 and 2010, respectively.

He worked with the Electrical and Computer Engineering Department at Illinois Institute of Technology, Chicago, as a Research Associate. Currently, he is a Postdoctoral Fellow with the Electrical Engineering Department Sharif University of Technology, Iran. His research interests include wide-area measurement system, reliability modeling and assessment, and smart grid technologies.

Dr. Aminifar is the Guest Editor of a Special Issue on Microgrids of the IEEE TRANSACTIONS ON SMART GRID. He received the IEEE Best Ph.D. Dissertation Award from Iran Section for his research on the probabilistic schemes for the placment of phasor measurement units.

Mahmud Fotuhi-Firuzabad (SM'99) received the B.Sc. degree in electrical engineering from Sharif University of Technology, Tehran, Iran, in 1986, the M.Sc. degree in electrical engineering from Tehran University, Tehran, in 1989, respectively, and the M.Sc. and Ph.D. degrees in electrical engineering from the University of Saskatchewan, Saskatoon, Canada, in 1993 and 1997, respectively.

Currently, he is a Professor and Head of the Department of Electrical Engineering, Sharif University of Technology. He is also an Honorary Professor in the Universiti Teknologi Mara (UiTM), Shah Alam, Malaysia.

Dr. Fotuhi-Firuzabad is a Member of the Center of Excellence in Power System Control Management and Control. He serves as an Editor of the IEEE TRANSACTIONS ON SMART GRID.

Mohammad Shahidehpour (F'01) is Carl Bodine Chair Professor and Director of Robert W. Galvin Center for Electricity Innovation at the Illinois Institute of Technology, Chicago. He is an Honorary Professor at Sharif University of Technology and the North China Electric Power University. He is the recipient of the 2009 Honorary Doctorate from the Polytechnic University of Bucharest.

Amir Safdarian (S'11) obtained the B.S. (Hon.) degree in electrical engineering from University of Tehran, Tehran, Iran, in 2008 and the M.S. (Hon.) degree in electrical engineering from Sharif University of Technology, Tehran, in 2010. He continued his studies there, where he is currently working toward the Ph.D. degree.

His research interests include reliability, vulnerability, and operation of power systems.